Journal of Nuclear Materials 386–388 (2009) 784–788

Contents lists available at ScienceDirect

Journal of Nuclear Materials

journal homepage: www.elsevier.com/locate/jnucmat

Characterization of thick plasma spray tungsten coating on ferritic/martensitic steel F82H for high heat flux armor

Y. Yahiro [a,*], M. Mitsuhara [a], K. Tokunakga [b], N. Yoshida [b], T. Hirai [c], K. Ezato [d], S. Suzuki [d], M. Akiba [d], H. Nakashima [a]

[a] Interdiscplinary Graduate School of Engineering Sciences, Kyushu University, Kasuga, Japan
[b] Research Institute for Applied Mechanics, Kyushu-u University, Kasuga, Japan
[c] IEF2 Forschungszentrum Juelich, Juelich, Germany
[d] Japan Atomic Energy Agency, Tokai, Japan

A B S T R A C T

Two types of plasma spray tungsten coatings on ferritic/martensitic steel F82H made by vacuum plasma spray technique (VPS) and air plasma spray technique (APS) were examined in this study to evaluate the possibility as plasma-facing armor. The VPS-W/F82H showed superior properties. The porosity of the VPS-W coatings was about 0.6% and most of the pores were smaller than 1–2 μm and joining of W/F82H and W/W was fairly good. Thermal load tests indicated high potential of this coating as plasma-facing armor under thermal loading. In case of APS-W/F82H, however, porosity was 6% and thermal load properties were much worse than VPS-W/F82H. It is likely that surface oxidation during plasma spray process reduced joining properties. Remarkably, both coatings created soft ferrite interlayer after proper heat treatments probably due to high residual stress at the interfaces after the production. This indicates the potential function of the interlayer as stress relieve and possible high performance of such coating component under thermal loads.

1. Introduction

Tungsten (W) is promising plasma-facing armor material in the future fusion devices. The advantage of W is the high melting point, low tritium inventory and low erosion rate under plasma loading [1,2]. The main drawbacks of W are the high ductile to brittle transition temperature (DBTT, approximately 400 °C) and difficulties in machining. A possible solution for the utilization of tungsten at plasma-facing surfaces is the coating of the heat sink or structural material with a thin tungsten layer. As coating technologies, vacuum plasma spray (VPS) [3], physical vapor deposition (PVD) [4,5] and chemical vapor deposition (CVD) [6], have been proposed and tested under high heat flux loading. As substrate materials for W coating, the following materials have been applied: copper or copper alloys foreseen in concern of water cooled system, graphite and/or CFC [7–10] for inertially cooled system and reduced activation ferritic steel [11]. In the present study, F82H ferritic/martensitic reduced activation steel, which is a leading structural material candidate for a fusion demonstration reactor, was selected as the substrate.

In this paper, characterization of thick plasma spray coatings of W on F82H steel and the evaluation of impacts of various heat treatments on the coating systems are presented.

2. Experimental procedures

Reduced activation ferritic steel substrate with dimension of 20 mm × 20 mm × 2.5 mm were coated by vacuum plasma splaying technique (VPS) and also by air plasma splay (APS). The substrate material was F82H, (Fe-8Cr-2W) developed by JAEA. Its thermal expansion and thermal conductivity at 300 K are $11.7 \times 10^{-6}\,K^{-1}$ and $0.82\,W/cm^{-1}\,K^{-1}$, respectively. After roughing the surface of the substrate by burst treatment for better adhesion, APS and VPS were performed at TOCALO Co. Ltd. in Japan. The thickness of the coating layer in both cases is 1.0 mm. In order to suppress oxidation and change of the ferritic/martensitic structure during the spraying processes, bulk temperature of the substrate was kept below 150 and 600 °C for APS and VPS, respectively. The average size of the W powders for APS and VPS were 40 and 17 μm, respectively.

In order to examine metallurgically, microstructure of the coatings and the substrate were observed by means of scanning electron microscopy (SEM), orientation imaging microscopy (OIM) and transmission electron microscopy (TEM). OIM gives the 2-D information of the orientation of each crystalline grains

* Corresponding author.
E-mail address: yahiro@riam.kyushu-u.ac.jp (Y. Yahiro).

0022-3115/$ - see front matter © 2009 Published by Elsevier B.V.
doi:10.1016/j.jnucmat.2008.12.219

and local strain. In order to obtain thin foil specimens of about 100 nm-thick for TEM observation, cross-sectional specimen preparation technique with a focused ion beam device (FIB) was used. Local hardness was measured by a nano-indenter.

Thermal response tests were carried out in the electron beam facility JUDITH [12,13]. Its maximum beam power is 60 kW and the beam diameter is 1 mm. The acceleration voltage of electron beam is 120 kV. A single color pyrometer (observing wavelength: around 1.5–1.6 μm) observes surface temperature in the area of 3–4 mm diameter at the surface though a quartz window with viewing angle of approximately 45°. The effective emissivity including transmission of the window was calibrated by the melting temperature of the W coating at 3400 °C.

3. Results

3.1. Structure

SEM micrographs in Fig. 1 show surface morphology of VPS-W and APS-W, and the corresponding cross-sectional structures. The surface of VPS-W has very fine rough structure. In addition, many spherical particles of about 20 μm or less, which probably have not melted perfectly during the plasma spray process, exist on the surface. Such very rough surface morphology indicates that the temperature of the melted particles was not high enough to form ideal pan cake-like depositions with smooth surface. On the other hand, the surface of the APS-W is smoother and the number of the un-melted particles is lower. These results indicate that the heating power of the plasma for VPS process was not high enough to form smooth surface. The cross-sectional SEM micrographs show that pores size is small in the VPS-W (less than 1–2 μm), in spite of the very rough surface. In case of APS-W, however, many pores larger than 10 μm remain. Reflecting the size of the pores, the porosity of VPS-W and APS-W estimated from the cross-sectional SEM micrographs were 0.6% and 6%, respectively. The low porosity of the VPS-W indicates that quite good thermo-mechanical properties would be expected.

In order to know the effects of the plasma spray on phase stability of the F82H, the cross-sectional samples of VPS/F82H and APS/F82H were observed by means of OIM. Typical inverse pole figure (IPF) images and misorientation maps at and near the interface of VPS-W/F82H and APS-W/F82H are shown in Fig. 2. In both case, distribution of the rotation angle between the neighboring grains estimated from the IPF images had peaks at 50° and 60°. This fact indicates that most of the crystalline grains are martensite. It means that the surface temperature was successfully suppressed not to exceed the phase transformation temperature from martensite to ferrite (770 °C). The misorientation map of VPS-W/F82H, however, shows that residual strain exists in the vicinity of the interface of about 20 μm. Micro-harness at this area measured by a nano-indenter was about two times higher than that of matrix.

Fig. 2 also shows that re-solidified pan cake-like depositions of W have columnar structure. The size of the columnar crystals in VPS-W is much smaller than those of APS-W. Relatively large round-shaped grains must be un-melted W powders, which are also visible in Fig. 1.

In order to know the details of the microstructure, very thin cross-sectional TEM specimens were picked up by using FIB. Fig. 3(a) shows a typical micrograph at the VPS-W/F82H interface. It is remarkable that no precipitations such as WC were formed at the interface and in the matrix. Excepting relatively large pores, joining properties looks rather good. Joining between the pan cake-like depositions also looks good, though fine pores less than 0.5 μm remains (see Fig. 3(b)). The columnar structure developed well where the two pan cake-like deposits join well, but not around large pores.

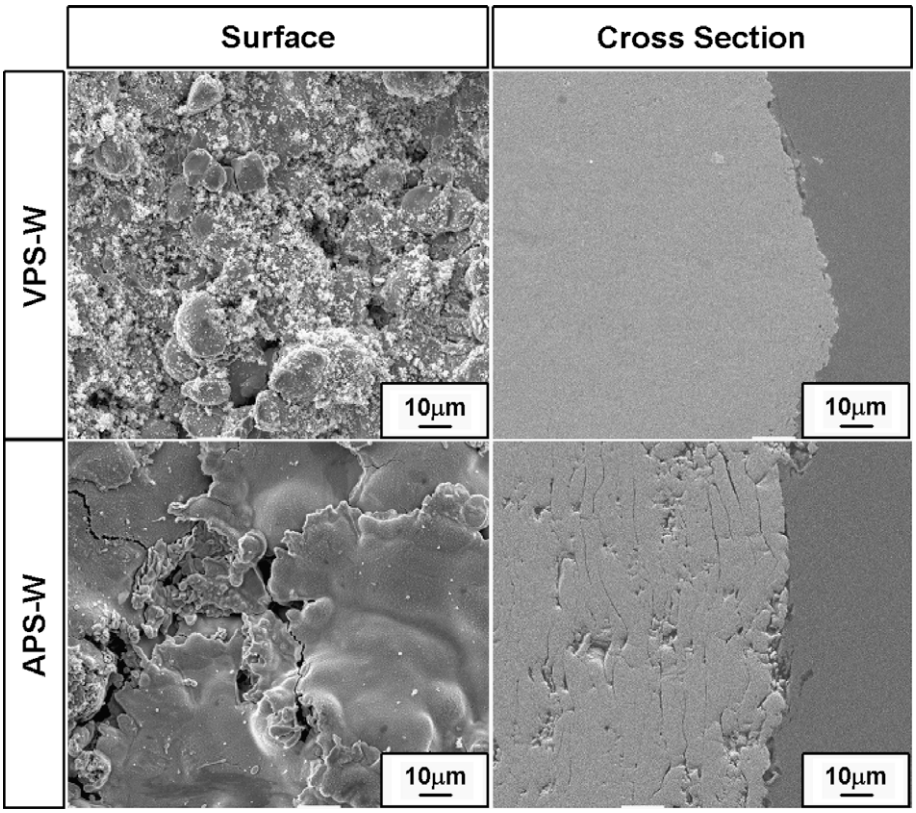

Fig. 1. SEM micrographs showing surface morphology of VPS-W and APS-W, and the corresponding cross-sectional structures.

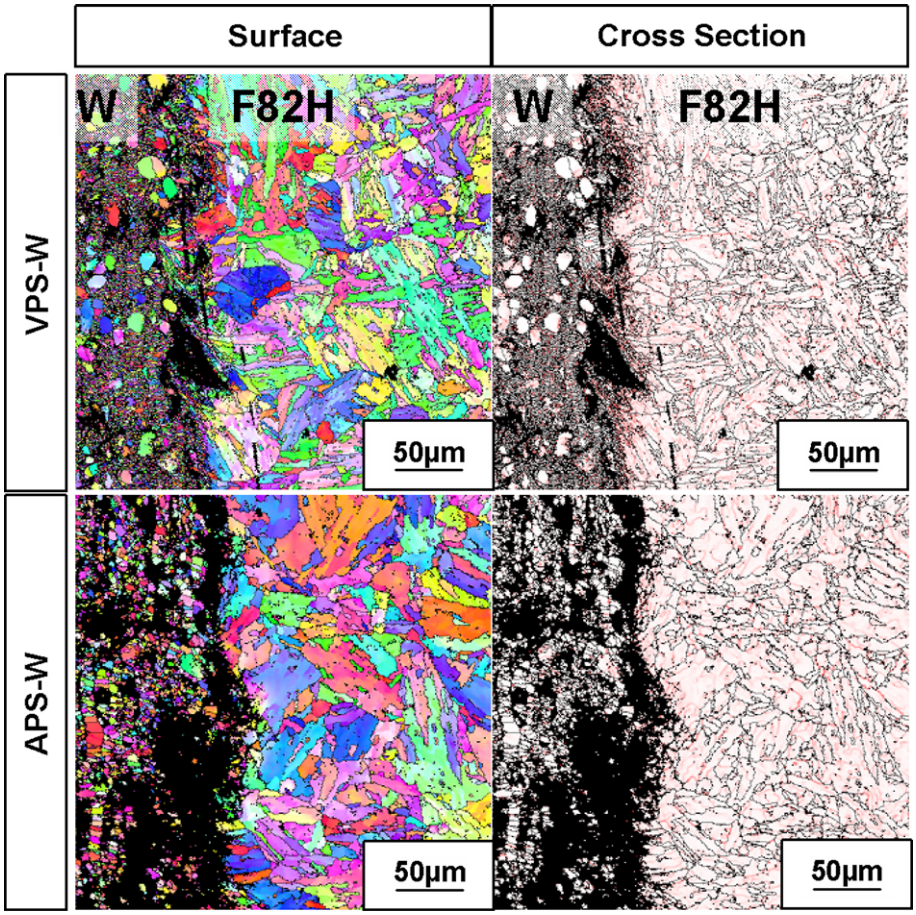

Fig. 2. Typical inverse pole figure images and misorientation maps at and near the interface of VPS-W/F82H and APS-W/F82H.

The experimental results mentioned above indicate that joining of W and F82H and also W and W in VPS-W/F82H is metallurgical good. Reduction of pores size less than 1 μm is a key issue for the material improvement.

3.2. Thermal response of the coatings

Thermal response tests were carried out in the electron beam facility JUDITH. Fairly homogenous distribution of heat deposition is realized by fast scanning of the electron beam. For the thermal response tests, moderate thermal impulses were applied for 1 ms. In this duration, the heat propagates in the range of characteristic heat propagation distance around 340 μm by assuming bulk W [14]. Note that the thermal diffusivity of W coating is smaller than bulk W, therefore, the distance is much shorter. This indicates that the thermal response tests reflect thermal properties of W coating (1-mm thick) but not those of the interface and substrate.

Fig. 4 shows surface temperature increases of APS-W, VPS-W coatings and a bulk W as a function of power density. The surface temperature of APS-W was significantly higher than the others. The temperature increase was fairly linear dependence as indicated in

$$\Delta T = 2P \times t^{0.5} \times (\pi \times \lambda \times \rho \times c)^{-0.5}, \quad (1)$$

where P stands for power density (W/m^2), t for time (s), λ for thermal conductivity (W/m/K), ρ for density (kg/m^3), and c for specific heat (J/kg/K). Comparing surface temperatures at a power density, it is possible to evaluate the ratio of material constants ($M \cong (\lambda \cdot \rho \cdot c)$). Consequently, the material constant of APS-W and VPS-W were estimated to be 17% and 58% of the bulk W. It shows clearly that VPS-W had higher performance than APS-W coating. It is likely that the inferior material constant of APS-W coating was caused by the higher porosity and high impurity content. The quality of the coatings still needs to be improved.

3.3. Thermal shock resistances of the coatings

The coatings were exposed to thermal shock loads in a range of 0.19 to 0.56 GW/m^2 for 5 ms in JUDITH facility. The surface temperature increases were very different between APS-W and VPS-W coating as expected from the thermal response test (Section 3.2). At the same power density, 0.19 GW/m^2, the increases were 2360 °C at APS-W coating and 1300 °C at VPS-W coating. Surface morphology after the thermal shock load tests are summarized in Fig. 5. The coatings of APS-W and VPS-W started to melt above 0.38 and 0.56 GW/m^2, respectively. They started to show cracking even lower power density, 0.19 and 0.38 GW/m^2. In any case, VPS-W coatings show better performance than APS-W coatings. Large holes at the re-solidified surface of APS-W indicated that large amount of gas have been retained in the coated W.

3.4. Heat treatments and its impact on W/F82H interface

In order to remove the internal stress remained in F82H near the interface, heat treatment was performed by taking into account

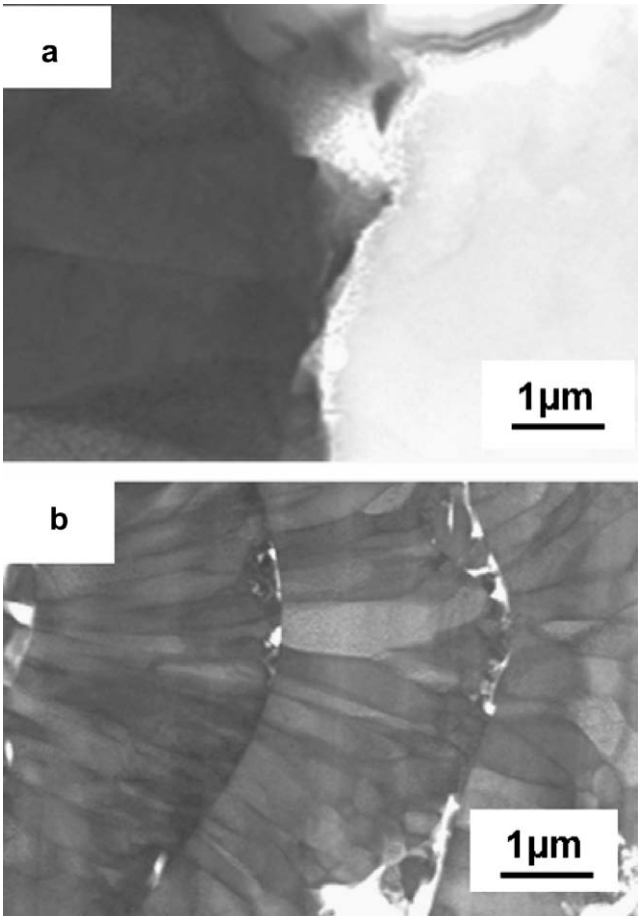

Fig. 3. TEM micrograph at VPS-W. (a) Interface, and (b) tungsten layer.

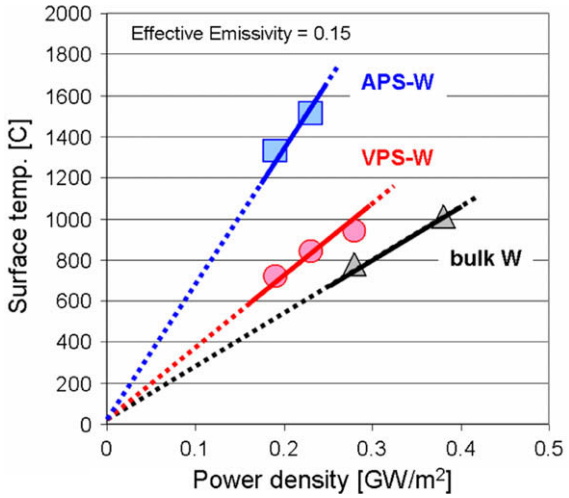

Fig. 4. Surface temperature of APS-W, VPS-W coatings and a bulk W as a function of power density.

the stability of the phase. The samples were heated at 960 °C for 0.5 h at first and then at 750 °C for 1.5 h in high vacuum. IFP map and misorientation map of VPS-W/F82H after the heat treatment are shown in Fig. 6. The ferritic phase with large grain size developed from the interface and residual strain at the interface disappeared simultaneously. The thickness of the ferritic phase is about 200–300 μm. The matrix of the F82H substrate became typical dual-phase structure of ferrite/martensite. On the other hand, formation of the ferritic phase layer did not occur by the two-step heat-treatment at 850 °C for 0.5 h and at 750 °C for 1.5 h.

It is worth to note that remarkable WC precipitations, which may reduce the joining strength, were not observed at the interfaces, in spite of the ferritic phase formation, namely in spite of the reduction of carbon content in the ferritic phase region. It is expected that softer ferritic phase at the interface will act as good interlayer which reduce misfit of the harder F82H substrate and W layer. It is important that the thickness of the ferritic phase layer can be controlled easily by changing the annealing time at 960 °C.

In case of APS-W/F82H, the thickness of the ferritic phase at the interface is about 500 μm for the heat treatment at 950 °C for 0.5 h followed by that at 750 °C for 1.5 h. In this material, unfortunately, many cracks between W layers are formed by the heat treatment.

4. Discussions

4.1. Optimization of the plasma spray conditions

APS method is very attractive because the technique is rather simple and thus application is wider. However, as described in Section 3.1 the porosity of APS-W/F82H is about 6%, which is one order higher than that of VPS-W/F82H. It is considered that this high porosity resulted in the weak heat load resistance as mentioned in Section 3.2 due to reduction of effective thermal conductivity. Plasma spray of melted W powders was performed by scanning the plasma gun on the substrate. It means that there was rather long time interval until the next scanning coming (about 1–2 s in the preset case). Therefore, the fresh surface of the deposited W will be oxidized quickly in air during the time interval. Once the remarkable oxidation occurred at the solid W surface, strong sticking of the melted droplets on the solid surface will become difficult and as a result large pores will be formed. It is considered that the application of APS technique will be limited for our purpose.

The preliminary thermal response test and thermal shock test described in Sections 3.2 and 3.3 indicate that VPS-W/F82H has considerably good heat load resistance, though more tests such as cyclic heat load test are required to evaluate the heat load resistance fully. The porosity of VPS-W/F82H is very low but it has still fine pores less than 1–2 μm as shown in the TEM micrographs of Fig. 3. In order to improve heat load resistance, one should know the mechanism of the fine pores formation at first. Very fine columnar crystal structure in pan cake-like depositions and very limited area with smooth surface comparing to the APS-W/F82H indicate that the temperature of the melted W powders was not high enough. Existence of un-melted round W crystals also indicated the insufficient heating power of plasma. If the temperature of the melted droplets of W is high enough, they can penetrate well into the fine holes and even shadows before re-solidification. It is expected that the porosity and adhesion strength can be improved by optimizing the powder side of W and plasma heating power.

4.2. Roles of ferritic layer at the interface

It is anticipated that locally induced residual strain and hardening during the plasma spray process in the F82H substrate near the interface may lead to the exfoliation of the W coating. Moreover, appropriate measures for large difference of thermal expansion of the materials are required, because the long life time of the coating under cyclic heat load is an important concern for fusion application. As described in Section 3.4, the two-step heat treatment at 960 and 750 °C is promising. It was shown that not only release of the residual strain but also formation of thin soft ferritic interlayer as stress relieve was possible. Residual strain at the interface

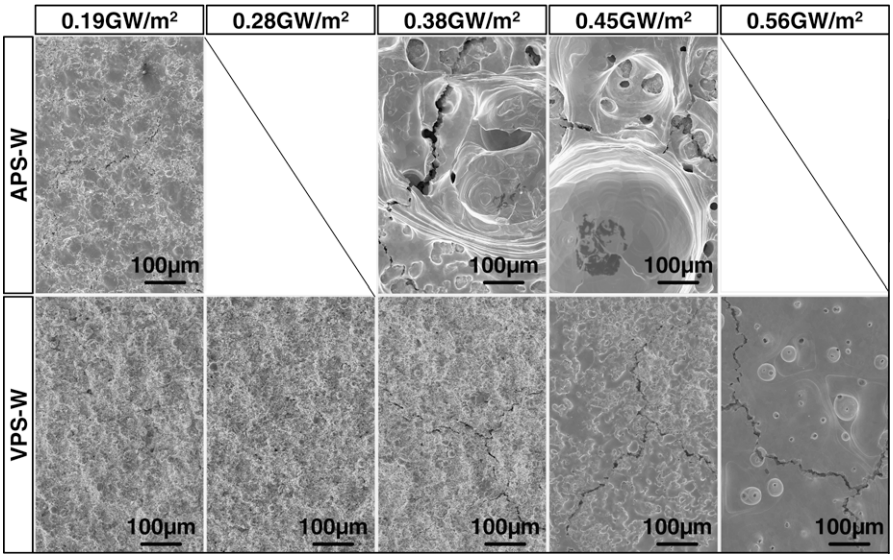

Fig. 5. Surface morphology after the thermal shock load tests.

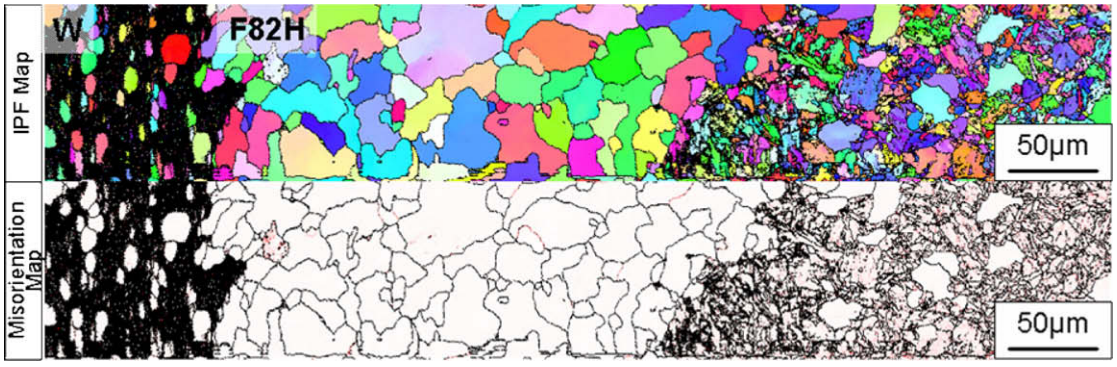

Fig. 6. IFP map and misorientation map of VPS-W/F82H after the heat treatment.

region and diffusion of carbon in F82H through the interface might be the driving force of the ferritic layer formation. Cyclic pulse heat load test is planned to evaluate the effects of the ferritic interlayer.

5. Summary

Two types of plasma spray tungsten coatings on ferritic/martensitic steel F82H made by vacuum plasma spray technique (VPS) and air plasma spray technique (APS) were examined in this study to evaluate their possibility as a plasma-facing armor.

The porosity of the VPS-W coatings was about 0.6%. The cross-sectional TEM observation showed that most of the pores were smaller than 1–2 μm and joining condition of W/F82H and W/W was fairly good. No remarkable carbides and oxides were observed at the interface. Thermal response test and thermal shock resistance tests indicated high potential of this coating as plasma-facing armor under thermal loading. For the reduction of fine pores usage of smaller W powders and/or increasing of power of plasma splay gun will be effective. In case of APS-W/F82H, porosity was 6% and heat load properties were much worse than VPS-W/F82H. It is likely that surface oxidation during plasma spray process deteriorated joining properties. Application of APS-W for a plasma-facing armor will be limited. Remarkably, both coatings created soft interlayer after proper heat treatments probably due to high residual stress at the interfaces after the production. This indicates the potential function of the soft interlayer as stress relieve and possible high performance of such coating component under thermal loads.

References

[1] G. Federici, C.H. Skinner, J.N. Brooks, J.P. Coad, C. Grisolia, A.A. Haasz, et al., Nucl. Fusion 41 (2001) 1967.
[2] I. Smid, M. Akiba, G. Vieider, L. Ploechl, J. Nucl. Mater. 258–263 (1998) 1602.
[3] S. Deschka, C. Garcia-Rosales, W. Hohenauer, R. Duwe, E. Gauthier, J. Linke, M. Lochter, W. Mallener, L. Plochl, P. Rodhammer, A. Salito, J. Nucl. Mater. 233–237 (1996) 645.
[4] H. Maier, J. Nucl. Mater. 335 (2004) 515.
[5] H. Maier et al., J. Nucl. Mater. 363–365 (2007) 1246.
[6] T. Hirai et al., Fus. Eng. Design 81 (2006) 175.
[7] K. Tokunaga, Y. Kubota, N. Noda, Y. Imamura, A. Kurumada, N. Yoshida, T. Sogabe, T. Kato, B. Schedler, Fus. Eng. Design 81 (2006) 133.
[8] K. Tokunaga, R.P. Doerner, R. Seraydarian, N. Noda, N. Yoshida, T. Sogabe, T. Kato, B. Schedler, J. Nucl. Mater. 307–311 (2002) 126.
[9] K. Tokunaga, N. Yoshida, Y. Kubota, N. Noda, Y. Imamura, A. Kurumada, T. Oku, T. Sogabe, T. Suzuki, T. Kato, L. Plöchl, J. Plasma Fus. Res. Ser. 3 (2000) 260.
[10] K. Tokunaga, N. Yoshida, N. Noda, K. Kubota, S. Inagaki, R. Sakamoto, T. Sogabe, L. Ploechl, J. Nucl. Mater. 266–269 (1999) 1224.
[11] H. Greuner, H. Bolt, B. Boeswirth, S. Lindig, W. Kuehnlein, T. Huber, K. Sato, S. Suzuki, Fus. Eng. Design 75–79 (2005) 333.
[12] R. Duwe, W. Kuehnlein, H. Muenstermann, Proceedings of the 18th Symposium on Fusion Technology (SOFT), Karlsruhe Germany, 1994, pp. 355.
[13] T. Hirai, K. Ezato, P. Majerus, Mater. Trans. 46 (2005) 412.
[14] T. Hirai, G. Pintsuk, Fus. Eng. Design 82 (2007) 389.